

Phase control of intermittency in dynamical systems

Samuel Zambrano,¹ Inés P. Mariño,¹ Francesco Salvadori,^{2,3} Riccardo Meucci,³ Miguel A. F. Sanjuán,¹ and F. T. Arecchi^{2,3}

¹*Nonlinear Dynamics and Chaos Group, Departamento de Ciencias de la Naturaleza y Física Aplicada, Universidad Rey Juan Carlos, Tulipán s/n, 28933 Móstoles, Madrid, Spain*

²*Departamento of Physics, Università di Firenze, Italy*

³*CNR–Istituto Nazionale di Ottica Applicata, Largo E. Fermi, 6 50125 Firenze, Italy*

(Received 4 May 2006; published 10 July 2006)

We present a nonfeedback method to tame or enhance crisis-induced intermittency in dynamical systems. By adding a small harmonic perturbation to a parameter of the system, the intermittent behavior can be suppressed or enhanced depending on the value of the phase difference between the main driving and the perturbation. The validity of the method is shown both in the model and in an experiment with a CO₂ laser. An analysis of this scheme applied to the quadratic map near crisis illustrates the role of phase control in nonlinear dynamical systems.

DOI: [10.1103/PhysRevE.74.016202](https://doi.org/10.1103/PhysRevE.74.016202)

PACS number(s): 05.45.Gg

I. INTRODUCTION

By modifying a control parameter, a chaotic attractor can touch an unstable periodic orbit inside its basin of attraction, inducing a sudden expansion. This phenomenon is known as an interior crisis [1,2]. Beyond the crisis, the system preserves a memory of the former situation, so a fraction of the time is spent in the region corresponding to the precrisis attractor, and during the rest of the time excursions around the formerly unstable periodic orbit take place. This behavior is known as crisis-induced intermittency [3].

Before the crisis, such excursions cannot take place unless noise or an external perturbation induces them. Recently [4], a feedback method to enhance or tame the intermittency has been devised. The strategy is to force the system with a feedback in which the “typical” frequency of the excursions is either filtered or enhanced. This method has been shown to be effective in a chaotic CO₂ laser, as described in Ref. [5]. We must point out that for another type of crisis, the boundary crisis [1,2], a technique has been recently devised [6] that allows us to keep the trajectories close to the chaotic saddle resulting from the destruction of the chaotic attractor.

On the other hand, several techniques to control chaos [7] have been proposed, including both feedback methods [the Ott-Grebogi-Yorke (OGY) technique being the most representative [8]] and nonfeedback methods. The former appear as more effective since they enable us to stabilize the system in any of the unstable periodic orbits that lie in the chaotic attractor. However, they require a fast and accurate response to work appropriately, thus nonfeedback methods can be more useful when such a response cannot be provided.

Nonfeedback methods traditionally make use of the effect of harmonic perturbations in the global dynamics, although nonharmonic perturbations can also have a great influence on the final state of a nonlinear system [9]. A nonfeedback method whose effectiveness has been proved in periodically driven chaotic systems is phase control of chaos [10–12]. In this control scheme, the control parameter is the phase difference ϕ between the main driving and a small harmonic perturbation that is applied to the system, either parametric or as an additional external forcing. It has been shown both numerically [10–12] and experimentally in a circuit [12] that an accurate choice of ϕ plays a crucial role in stabilizing the dynamics of the system.

In this paper, we show that the intermittency at an interior crisis in a dynamical system can be controlled by a phase control scheme. We give experimental and numerical evidence of the validity of the method for the CO₂ laser close to an interior crisis. We show that, if we apply a small harmonic perturbation to the laser, an accurate selection of ϕ allows us to place the laser in the desired dynamical state, which can be either the intermittent regime or the precrisis regime. Three different values of the frequency of the perturbation are used: the frequency of the main forcing, f_0 , the frequency of the period doubling bifurcation, $f_0/2$, and, finally, $f_0/3$, which is the frequency of the unstable orbit responsible for the interior crisis. In order to have a deeper insight into the role of ϕ , we also present an analysis of phase control of the quadratic map close to a crisis and we show that ϕ influences drastically the global dynamics of the system. All this evidence confirms that the phase ϕ plays an important role in the final state of the system, so it can be used to control the intermittency.

The structure of the paper is as follows. In Sec. II, we describe the laser and the phase control scheme. In Secs. III and IV, we show the effectiveness of the method in controlling the intermittency when the unperturbed laser is operating before and after the crisis, respectively. The phase control of the quadratic map is presented in Sec. V. Finally, Sec. VI is devoted to the conclusions.

II. EXPERIMENTAL SETUP AND IMPLEMENTATION OF THE PHASE CONTROL SCHEME

The experimental setup consists of a single-mode CO₂ laser, as shown in Fig. 1. The laser cavity is defined by a totally reflecting grating and a partially reflecting mirror (G and M), and the gain medium is pumped by a constant electric discharge current. An electro-optic modulator (EOM) is inserted in the laser cavity in order to control the cavity losses by an external forcing, obtained from a sinusoidal generator (MD), that can be represented as

$$F(t) = \beta \sin(2\pi f_0 t) + b_0, \quad (1)$$

where β is the amplitude of the external forcing, b_0 is a bias voltage, and $f_0 = 100$ kHz is about twice the relaxation frequency of the laser.

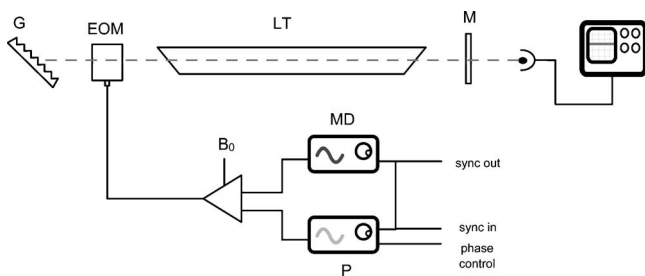


FIG. 1. Experimental setup for a single-mode CO₂ laser with modulated losses. EOM, intracavity electro-optic modulator; G, total reflecting grating; M, partial reflecting mirror; D, fast infrared detector; P, sinusoidal generator; MD, digital oscilloscope.

The CO₂ modulated laser is accurately described by the following model of five differential equations [13]:

$$\begin{aligned}
 \dot{x}_1 &= kx_1\{x_2 - 1 - \alpha \sin^2[F(t)]\}, \\
 \dot{x}_2 &= -\gamma_1 x_2 - 2kx_1 x_2 + gx_3 + x_4 + p, \\
 \dot{x}_3 &= -\gamma_1 x_3 + gx_2 + x_5 + p, \\
 \dot{x}_4 &= -\gamma_2 x_4 + zx_2 + gx_5 + zp, \\
 \dot{x}_5 &= -\gamma_2 x_5 + zx_3 + gx_4 + zp.
 \end{aligned} \tag{2}$$

In the above equations, x_1 represents the laser output intensity, x_2 is the population inversion between the two resonant levels, and x_3 , x_4 , and x_5 account for molecular exchanges between the two levels resonant with the radiation field and the other rotational levels of the same vibrational band. The parameters of the model are the following: k is the unperturbed cavity loss parameter, g is a coupling constant, γ_1 and γ_2 are population relaxation rates, z accounts for an effective number of rotational levels, α accounts for the efficiency of the electro-optic modulator, and p is the pump parameter. The rest of the parameters are related to the external periodic forcing defined above.

By increasing the amplitude of the external forcing, the system undergoes a sequence of subharmonic bifurcations, and for $\beta < 0.1$ the dynamics is restricted to a certain region of the phase space, say $|x_1| < 0.013$, as shown in Fig. 2. Further increase of β induces an interior crisis. This leads to the occurrence of a regime where there is an intermittency between orbits contained in the precrisis bounding region and excursions out of it, of period 3 and 4. The set of parameters used in the numerical simulations is $k=30$, $\alpha=4$, $\gamma_1=10.0643$, $g=0.05$, $p=0.01987$, $\gamma_2=1.0643$, $z=10$, $f_0=1/7$, and $b_0=0.1794$. The stability analysis provides a value of the relaxation oscillation frequency of 0.07, which is around half the frequency of the forcing signal.

Let us now describe the *phase control scheme*. First, we perturb harmonically one of the parameters of the system. We choose b_0 because it is easily accessible in the experimental setup. The perturbed parameter becomes a periodic function $b(t)=b_0[1+\epsilon \sin(2\pi f_0 r t + \phi)]$, where ϵ is the perturbation amplitude, r is the resonance condition, and ϕ is the phase difference. The phase control scheme relies on an ap-

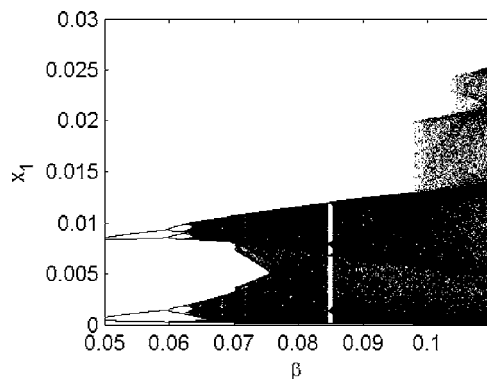


FIG. 2. Numerical bifurcation diagram for β . Two interior crises are observed, but we are going to study the effect of harmonic perturbations on the laser around the first crisis.

propriate use of the phase ϕ , once ϵ and r are fixed.

Due to the fact that $F(t)$ depends linearly on the bias b_0 , one can clearly see that adding a harmonic perturbation to the bias is equivalent to adding a second periodic forcing, which is one of the possible implementations of the phase control scheme [10,11]. Thus, for the perturbed system, the forcing term of Eq. (2) should read

$$F(t) = \beta \sin(2\pi f_0 t) + \epsilon' \beta \sin(2\pi f_0 r t + \phi) + b_0, \tag{3}$$

with $\epsilon' = b_0 \epsilon / \beta$. We consider ϵ' instead of ϵ , since it enables us to quantify the strength of the applied perturbation in terms of the main periodic forcing.

III. PHASE CONTROL OF THE LASER IN A PRECRISIS REGIME

We consider the role of the phase when the unperturbed laser is placed in the situation previous to the interior crisis, so that no intermittency takes place (not even induced by noise, since we choose to be quite far from the interior crisis). In this case, we characterize the effect of ϕ for fixed values of ϵ' and r by taking records of very long time series where ϕ is slowly varied $\phi \mapsto \phi(t) = 2\pi \mu t$, where $\mu \ll 1/f_0$, i.e., the phase varies very slowly compared to the typical time scale of the laser. Thus, for $t=0$ the phase difference is $\phi=0$ and it increases until $t=1/\mu$, where it is $\phi=2\pi$. The dynamical state of the system at a certain time t' corresponds essentially to the expected behavior for $\phi=2\pi \mu t'$.

Let us first analyze the case in which the frequency of the perturbation is the same as the frequency of the main driving, that is, $r=1$. The experimental long time series for this case is plotted in Fig. 3. We can observe how there is an increase of the amplitude of the peaks when ϕ is close to 0 and 2π , and a depression as ϕ goes to π . This phenomenon has a simple explanation,

$$\begin{aligned}
 F(t) &= \beta \sin(2\pi f_0 t) + \epsilon' \beta \sin(2\pi f_0 t + \phi) \\
 &= \beta' \sin(2\pi f_0 t + \phi_0),
 \end{aligned} \tag{4}$$

where

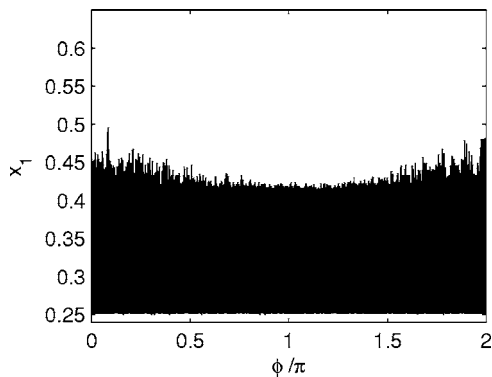


FIG. 3. Long time series varying the phase ϕ for $r=1$, $\epsilon'=0.1$. Note that for $\phi=0$ and 2π , the maxima of the series are increased, as expected.

$$\beta' = \beta\sqrt{1 + \epsilon'^2 + 2\epsilon'\cos\phi}. \quad (5)$$

Notice that we basically have a single forcing, so the resulting ϕ_0 plays an irrelevant role. However, the effective amplitude of the perturbation, β' , depends on ϕ . Thus, by choosing $\phi=0$, the effective amplitude of the periodic forcing is increased to a value closer to the critical value so the height of the peaks becomes bigger. Instead, by choosing $\phi=\pi$, β' becomes smaller, so the system is farther away from the crisis, and the height of the peaks becomes smaller. We shall point out, in this figure, that with a perturbation of about 10% of the main forcing, the system is not led to the intermittent regime. This is not very relevant by itself, because Eq. (5) shows that the necessary amplitude of the perturbation to lead the system to the intermittent regime could be reduced just by placing the unperturbed system closer to the crisis. However, it is an important reference to evaluate the effectiveness of perturbations with different frequencies.

Now we consider the laser in the same unperturbed situation before the crisis and we apply a perturbation whose frequency is the same as the frequency of the unstable periodic orbit involved in the interior crisis [4], that is, $f_0/3$. The two main behaviors observed experimentally are summarized in the two diagrams shown in Fig. 4. We observe an evident $2\pi/3$ symmetry of the first diagram, which could be deduced from the invariance of Eq. (3) under the transformation $t \rightarrow t + k/f_0$ and $\phi \rightarrow \phi + 2\pi rk$, with k an integer. Figure 4(a) shows the crucial role played by the phase difference. For the same values of the perturbation amplitude, by adjusting the phase, the system can be placed either in an intermittent regime or in the precrisis regime. It is important to note that we observe experimentally this significant effect even if the amplitude of the perturbation applied is about 0.3% of the amplitude of the main forcing, which is much smaller than in the $r=1$ case. However, as we observe in Fig. 4(b) for $\epsilon'=0.006$, there is intermittency for nearly all values of ϕ . In summary, the $r=1/3$ perturbation is much more effective than the $r=1$ perturbation to control the intermittency.

New features arise when the system is perturbed with the frequency corresponding to the period doubling bifurcation of the system, $f_0/2$. Again, two experimental diagrams are presented to see the effect of the phase, shown in Fig. 5. We

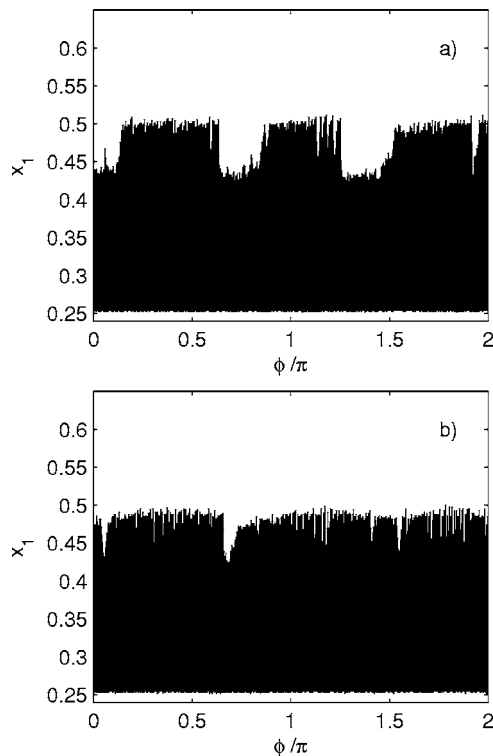


FIG. 4. Long time series varying the phase ϕ for $r=1/3$, $\epsilon'=0.003$ (a) and $\epsilon'=0.006$ (b). The diagrams present the expected $2\pi/3$ symmetry, even if in (b) the intervals of ϕ leading to intermittency have merged and the behavior is nearly phase-independent.

can observe the expected π symmetry in ϕ . On the other hand, Fig. 5(a) shows again that the phase difference modulates the maximum height of the peaks, but intermittency does not take place. However, when the perturbation is increased to $\epsilon'=0.01$, Fig. 5(b), just 1% of the main forcing, the effect of the phase is even clearer: again, the phase enables us to place the system either in the intermittent regime or in the small chaos regime. In the intermittent regime observed in Fig. 5(b), the high-amplitude orbits are related with the second interior crisis shown in Fig. 2, thus a variety of dynamical behaviors is accessible by varying ϕ .

Numerical calculations provide a confirmation of these results, together with a deeper insight into the role of the phase. A good indicator to discriminate between the different dynamical states of the laser for different values of the parameters is

$$\langle H \rangle = \langle \max(x_1(t)) \rangle_{|x_1(t) > x_0}, \quad (6)$$

where $\langle \cdot \rangle$ indicates the average over a long time series, and $\max(\cdot)$ indicates the relative maximum of the series. The value of x_0 is chosen in such a way that $\langle H \rangle$ enables us to distinguish between the small chaos and the intermittent regime. In the numerical simulations, we have observed that taking $x_0=10^{-5}$, that is, neglecting only the extremely small peaks of the signal, is sufficient for this discrimination. We have observed that $\langle H \rangle \leq 0.006$ corresponds to the precrisis chaotic regime, $0.006 < \langle H \rangle \leq 0.0074$ matches with the inter-

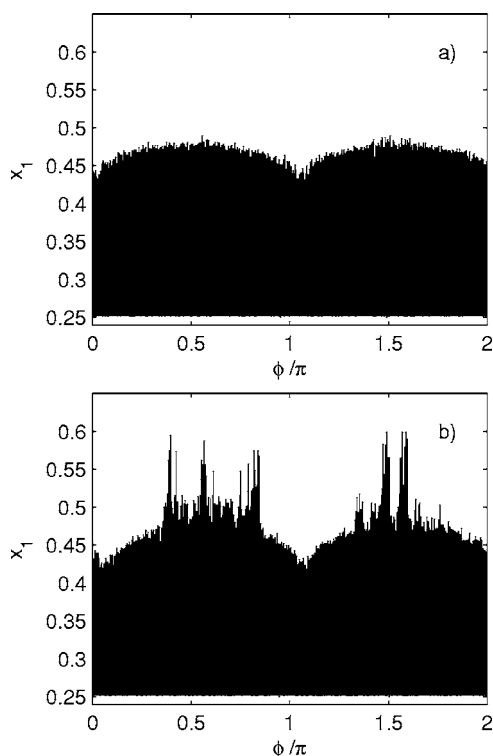


FIG. 5. Long time series varying the phase ϕ for $r=1/2$, $\epsilon'=0.006$ (a) and $\epsilon'=0.01$ (b). We have a π symmetry, as expected. The dependence on the phase ϕ is clear, and we observe that in (b) a correct selection of the phase determines whether there is intermittency.

mittent regime observed after the first crisis shown in Fig. 2, and $\langle H \rangle > 0.0074$ corresponds to the regime in which there are high-amplitude orbits, like those observed in Fig. 2 after the second crisis. $\langle H \rangle$ can be easily computed by numerical integration of the equations of the laser. We study the dependence of the global dynamics on the parameters of the system by calculating $\langle H \rangle$ as a function of ϵ and ϕ , fixing r .

Numerical calculations are presented in Fig. 6. As for the experimental results, we include the calculations for the trivial case $r=1$ for the sake of clarity. In this case, Fig. 6(a), the color of the diagram and thus $\langle H \rangle$ changes smoothly as the parameters vary, from a minimum at $\phi=\pi$ to a maximum at $\phi=0$ and 2π , as observed in the experiment (Fig. 3).

For the $r=1/3$ case, Fig. 6(b), $\langle H \rangle$ presents the expected $2\pi/3$ symmetry. On the other hand, it can be clearly observed how the value of $\langle H \rangle$ increases gradually with ϵ . For a narrow interval of ϵ , approximately $\epsilon \in [0.002, 0.003]$, depending on ϕ we have values of $\langle H \rangle$ bigger than 0.006 intercalated with values of $\langle H \rangle$ smaller than 0.006. This agrees with the phase-induced transitions between the intermittency and the small chaos regime observed experimentally. However, as in the experiment, we can see that if the perturbation amplitude ϵ is further increased, the intervals of ϕ giving rise to intermittency merge, so intermittency is observed almost independently of the phase.

Let us finally comment on the results for the $r=1/2$ case. For small values of ϵ , $\epsilon < 0.02$, the $\langle H \rangle$ remains around $\langle H \rangle \approx 0.005$ almost independently of the phase. However,

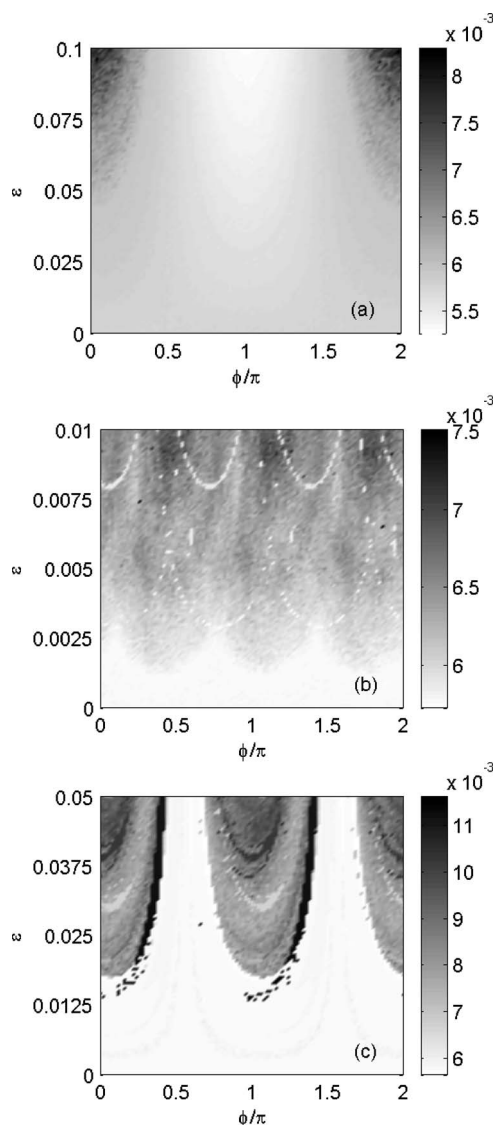


FIG. 6. The medium height of the maxima of x_1 , $\langle H \rangle$, as a function of ϵ and ϕ for $r=1$ (a), $r=1/3$ (b), and $r=1/2$ (c).

when ϵ becomes bigger than a certain critical value $\epsilon_0 \approx 0.02$, there is a sudden change in the medium height of the peaks. This sudden transition to a high $\langle H \rangle$ regime, which corresponds to the dynamical state observed after the second crisis of the laser, is evident from the drastic change of color that we can observe in the diagram of Fig. 6(c), which is fully consistent with the experiments on the laser. Thus, once again we see the important role played by ϕ in placing the system before or after the interior crisis.

IV. PHASE CONTROL OF THE INTERMITTENCY AFTER THE CRISIS

Up to now we have shown that the intermittency of the CO₂ laser in the precrisis regime can be controlled, by just varying the phase ϕ . In this section, in analogy with [4], we show that phase control also works when the unperturbed laser is placed in the post-crisis region.

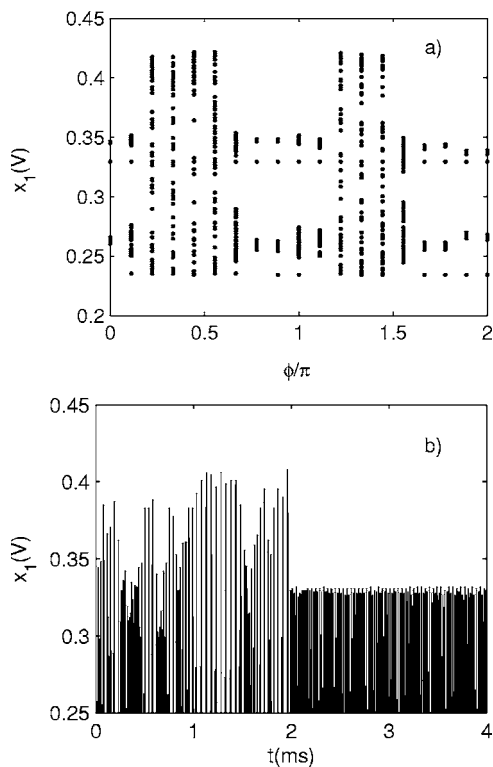


FIG. 7. Experimental bifurcation diagram (a), showing how an appropriate selection of the phase ϕ can take the laser from an intermittent regime to a small chaos regime. (b) A controlled time series of the laser, where control is applied at $t \approx 2$ ms and the intermittent behavior is nearly immediately suppressed.

In order to characterize the role of ϕ in this case, we have opted to perform a bifurcation diagram by localizing the maxima of different time series of the laser with different values of ϕ , for $\epsilon=0.01$ and $r=1/2$, as shown in Fig. 7(a). We can clearly appreciate a π symmetry in the diagram as in the previous section. We can see how a variation of ϕ allows us to move from the intermittent regime to the small chaos regime. The action of the applied perturbation on the laser is illustrated by Fig. 7(b), where we can see how, once the perturbation is applied (for $t \approx 2$ ms), the system passes from an intermittent regime, with the characteristic large spikes, to a small chaos regime.

We have performed a numerical analysis to see this phenomenon in more detail. We characterize the role of the phase ϕ by calculating $\langle H \rangle$, defined as in Eq. (6), and the results are shown in Fig. 8. Again, the symmetry induced by our selection of r and the nontrivial role played by the phase ϕ are evident.

Thus, we have shown that we can use ϕ to control the intermittency after the interior crisis.

V. PHASE CONTROL OF THE INTERMITTENCY IN THE QUADRATIC MAP

In order to gain a deeper insight into the role of ϕ in nonlinear systems, we study phase control in a paradigmatic nonlinear map close to an interior crisis. Our approach is

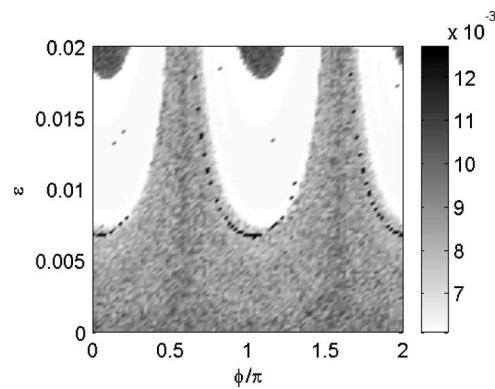


FIG. 8. The medium height of the maxima of x_1 , $\langle H \rangle$, as a function of ϵ and ϕ for $r=1/2$.

quite different from that of other authors [14,15], who have studied chaos control by harmonic perturbations in maps. Here we identify the key ingredients involved in the interior crisis for the unperturbed system. After this, we perform a perturbative analysis to estimate how these ingredients are affected by the presence of a periodic perturbation, thus emphasizing the nontrivial role played by ϕ .

We consider the unperturbed quadratic map given by

$$x_{n+1} = C - x_n^2 = F(C, x_n), \quad (7)$$

a paradigmatic system that is conjugate to the well known logistic map [16], and whose interior crisis has been extensively studied [1–3] even when two of these maps are coupled, a situation that has been related with chaotic itinerancy [17]. For this system, at $C=C_s \approx 1.76$, a stable period-3 orbit is born, a phenomenon referred to as subduction. If we increase the parameter C , there is a period-doubling bifurcation giving rise to three chaotic bands, but, after a critical value $C^* \approx 1.79$, the bands touch the unstable period-3 orbit that lies in its basin of attraction and they disappear. As a consequence, a one-piece chaotic attractor is obtained. This process is summarized in the bifurcation diagram shown in Fig. 9(a).

We are interested in the form of $F^3(C, x) \equiv F(C, F(C, F(C, x)))$ close to the crisis. It is depicted in Fig. 9(b) for $C \approx C^*$, together with the three points of the unstable period-3 orbit involved in the crisis x_i which verify $F^3(C, x_i) = x_i$, where the subindex i will be a , b , or c throughout this discussion. If we make a zoom of $F^3(C, x)$ close to each of the unstable periodic orbits, we can see that we have three small unimodal maps (inverted or reflected, but equivalent), whose structure is sketched in Fig. 9(c). Each of them is associated with one of the three chaotic bands and they can be essentially characterized by the unstable orbit x_i , the limit point $x_{L,i}$ which verifies $F^3(C, x_{L,i}) = x_i$ [see Fig. 9(c)], and the maximum $x_{m,i}$, for which $dF^3(C, x)/dx|_{x_{m,i}} = 0$. The values of $x_{m,i}$ that can be calculated analytically, and the values of $x_i, x_{L,i}$ that can be calculated using the Newton-Raphson method [18], will depend on C . The key idea that we want to illustrate is that the existence of the three bands for $C \leq C^*$ and their disappearance at $C > C^*$ can be interpreted in terms of the evolution of the three unimodal maps that are present

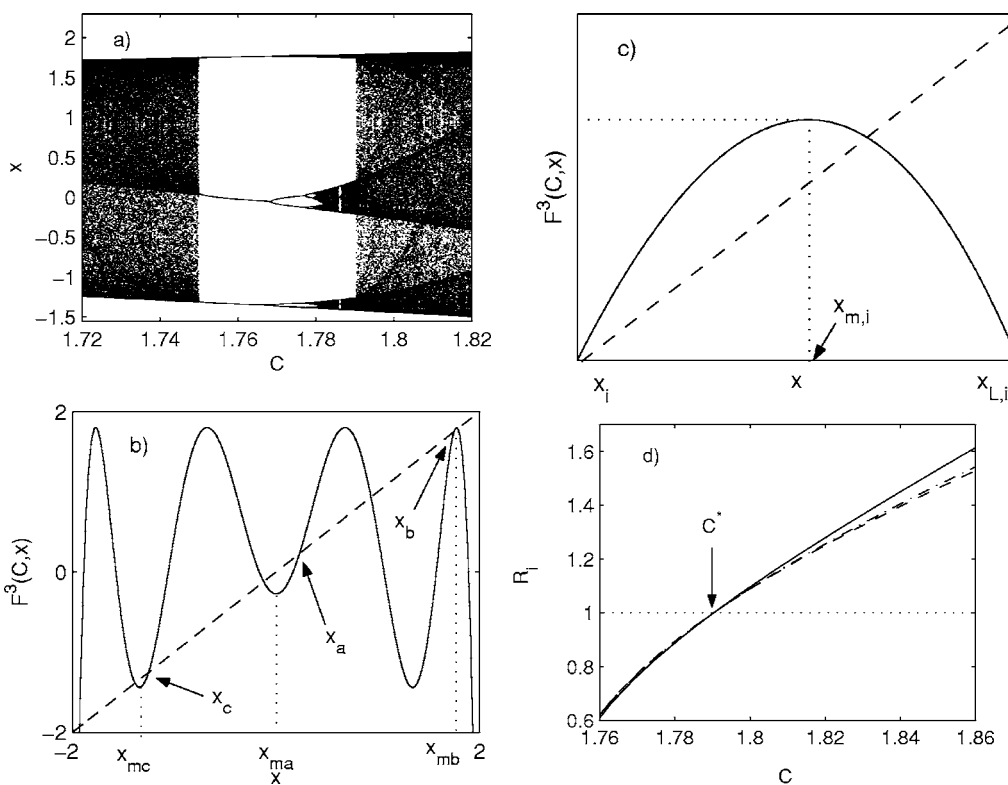


FIG. 9. (a) Bifurcation diagram showing the interior crisis for the quadratic map. (b) Plot of $F^3(C,x)$ as a function of x for $C \approx C^*$, where the unstable orbit x_a, x_b, x_c is marked. (c) Scheme of each of the three copies of a unimodal map present in $F^3(C,x)$, responsible for the three bands observed in the bifurcation diagram. (d) Plot of the numerical calculations of the three ratios R_i , $i \in \{a,b,c\}$, which are smaller than 1 for $C < C^*$ and bigger than 1 for $C > C^*$.

in $F^3(C,x)$. In fact, we claim that the bands will exist if these copies of a unimodal map present in $F^3(C,x)$ “trap” the orbits passing by $[x_i, x_{L,i}]$ (or $[x_{L,i}, x_i]$) under iterations of $F^3(C,x)$. Whether those three copies are “trapping” can be characterized by the following three ratios:

$$R_i(C) = \frac{|F^3(C, x_{m,i}) - x_i|}{|x_i - x_{L,i}|}, \quad i \in \{a,b,c\}. \quad (8)$$

It is easy to see that the bands will exist if $R_i \leq 1$, and they will disappear for $R_i > 1$. Thus, we claim that the ratios $R_i(C)$ will go from values smaller than 1 for $C < C^*$, before the crisis, to values larger than 1 for $C > C^*$, after the crisis. Numerical calculations of these ratios R_i as functions of C have been carried out and are shown in Fig. 9(d). Notice that the value of C^* obtained in this way corresponds to the one obtained in [1,2].

Bearing this in mind, we can now focus on the role of the phase ϕ when applying a harmonic perturbation to the system given by Eq. (7). Consider the perturbed map

$$x_{n+1} = C_n - x_n^2 = F(C_n, x_n), \quad (9)$$

where

$$C_n = C[1 + \epsilon \sin(2\pi r n + \phi)]. \quad (10)$$

We will assume $\epsilon \ll 1$. In analogy with the laser, it is easy to see that the $r=1$ case is quite trivial, because, by varying the

phase, we are just moving in C in the interval $[C(1 - \epsilon), C(1 + \epsilon)]$.

Instead, in the $r=1/3$ case the role of ϕ is far from being trivial. In this situation, the global dynamics will be governed by the autonomous map,

$$x_{n+3} = F(C_2, F(C_1, F(C_0, x_n))) \equiv G(x_n). \quad (11)$$

The smallness of ϵ will make $G(x_n)$ quite similar to $F^3(C, x_n)$. Thus, if $C \approx C^*$, $G(x)$ will also contain three small unimodal maps, and our aim is to see how the perturbed ratios R'_i of each of them vary with ϕ , where i again can be a, b , or c . First, it is straightforward to verify that the maxima of the perturbed system, $x'_{m,i}$, exist for ϵ sufficiently small, and can be written as

$$x'_{m,a} = 0,$$

$$x'_{m,b} = \sqrt{C_1 + \sqrt{C_0}},$$

$$x'_{m,c} = -\sqrt{C_0}.$$

Thus,

$$G(x'_{m,a}) = C_2 - (C_1 - C_0^2)^2,$$

$$G(x'_{m,b}) = C_2,$$

$$G(x'_{m,c}) = C_2 - C_1^2.$$

The values of the perturbed periodic orbit x'_i , verifying $G(x'_i) = x'_i$, can be approximated starting from the unperturbed ones (x_i) by means of the implicit function theorem (IFT) [19]. It is relatively simple to verify using this theorem that the order ϵ approximation is given by

$$x'_i \approx x_i - \epsilon \frac{C \sin(\phi)}{2x_i}. \quad (12)$$

Analogously, we can calculate the values of the perturbed $x'_{L,i}$ from the unperturbed $x_{L,i}$ by making use of the IFT. It can be shown quite easily that

$$x'_{L,i} \approx x_{L,i} - \epsilon \frac{C \sin(\phi)}{2x_{L,i}} \left(1 - \frac{1}{8F^2(C, x_{L,i})F(C, x_{L,i})} \right) \quad (13)$$

for $i \in \{a, b, c\}$. With the exact expressions obtained for $G(x'_{m,i})$ and the approximations of x'_i and $x'_{L,i}$ shown above, we can then approximate the new perturbed ratios,

$$R'_i(C, \epsilon, \phi) = \frac{|G(x'_{m,i}) - x'_i|}{|x'_i - x'_{L,i}|}. \quad (14)$$

Fixing ϵ and C , the three ratios will clearly depend on ϕ , so $R'_i = R'_i(\phi)$. We can see a bifurcation diagram and a plot of our approximations of $R'_i(\phi)$ in Fig. 10 for $C=1.8$ (the unperturbed system displays intermittency) and $\epsilon=0.005$. We can observe in the bifurcation diagram of Fig. 10(a) that the value of ϕ determines whether the system displays intermittency. On the other hand, we can see in Fig. 10(b) that the interval of ϕ for which there is intermittency corresponds roughly with the small interval around $\phi = \pi/2$ for which our approximations of the three ratios are bigger than 1. In this region, none of the copies of the unimodal map present in $G(x)$ are “trapping,” so the orbits are not restricted to any band and there is intermittency. Thus, our calculations provide a way to understand the nontrivial role of ϕ in the global dynamics of the system that matches with the numerical simulations.

Summarizing, we have seen that varying ϕ modulates both the geometry of the system and the position of the periodic orbit involved in the interior crisis. Thus, when we are close to the crisis, its contribution becomes crucial.

VI. CONCLUSIONS

We have shown that the phase control scheme is able to control the intermittency in a chaotic system close to an interior crisis. First, we have shown both experimentally and numerically how, if we apply a harmonic perturbation to a chaotic CO₂ laser, it is possible to control the crisis-induced intermittency by accurately choosing ϕ . We have seen that this scheme is more effective when the frequency of the perturbation is equal to either the frequency of the unstable periodic orbit involved in the crisis or the frequency involved in the period-doubling bifurcation, which can be obtained from experimental time series by using the Fourier transform. On the other hand, with the aid of the simple quadratic map, we have illustrated the nontrivial role that the phase

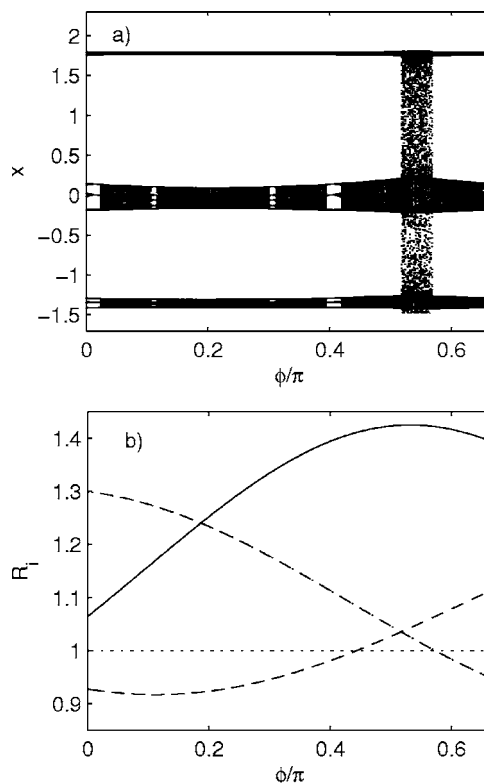


FIG. 10. (a) Bifurcation diagram of $G(x)$ for $C=1.8$, $\epsilon=0.005$ as a function of ϕ , showing that the value of the phase influences greatly whether there is intermittency. (b) Graphs of our approximation of the perturbed ratios R'_i as a function of ϕ : the ϕ interval where the intermittency is observed corresponds roughly to the interval for which $R'_i > 1$, as claimed.

difference ϕ plays when applying a harmonic perturbation to a dynamical system. Our analysis shows that the application of a periodic modulation to a system close to an interior crisis perturbs its geometry, and such perturbation depends strongly on ϕ , which becomes a key parameter for the global dynamics.

One important advantage of this scheme is its nonfeedback nature. Furthermore, the key role of the phase in selecting the final dynamical state is very useful from a control point of view, since there is a large variety of situations in which the modulation of the accessible parameters might be limited, and ϕ is an additional degree of freedom that may be very useful. To our knowledge, this is the first time in which it is shown numerically, experimentally, and analytically that the phase difference ϕ plays a key role not only to suppress chaos, but also to control the intermittency in chaotic systems close to a crisis. This makes the phase control scheme very versatile and useful in a wide variety of dynamical situations.

ACKNOWLEDGMENTS

This work has been financially supported by the Spanish Ministry of Science and Technology under Project No. BFM2003-03081 and by Acci3n Integrada Hispano-Italiana HI03-207, and also by FIRB Contract No. RBAU01B49F-002 and by Azione Integrata Italia Spagna IT1348.

- [1] C. Grebogi, E. Ott, and J. A. Yorke, *Phys. Rev. Lett.* **48**, 1507 (1982).
- [2] C. Grebogi, E. Ott, and J. A. Yorke, *Physica D* **7**, 181 (1983).
- [3] C. Grebogi, E. Ott, F. Romeiras, and J. A. Yorke, *Phys. Rev. A* **36**, 5365 (1987).
- [4] R. Meucci, E. Allaria, F. Salvadori, and F. T. Arecchi, *Phys. Rev. Lett.* **95**, 184101 (2005).
- [5] R. Meucci, D. Cinotti, E. Allaria, L. Billings, I. Triandalf, D. Morgan, and I. B. Schwartz, *Physica D* **189**, 70 (2004).
- [6] J. Aguirre, F. d'Ovidio, and M. A. F. Sanjuán, *Phys. Rev. E* **69**, 016203 (2004).
- [7] T. Shinbrot, C. Grebogi, E. Ott, and J. Yorke, *Nature (London)* **363**, 411 (1993).
- [8] E. Ott, C. Grebogi, and J. A. Yorke, *Phys. Rev. Lett.* **64**, 1990 (1990).
- [9] M. A. F. Sanjuán, *Phys. Rev. E* **58**, 4377 (1998).
- [10] Z. Qu, G. Hu, G. Yang, and G. Quin, *Phys. Rev. Lett.* **74**, 1736 (1995).
- [11] J. Yang, Z. Qu, and G. Hu, *Phys. Rev. E* **53**, 4402 (1996).
- [12] S. Zambrano, S. Brugioni, E. Allaria, I. Leyva, M. A. F. Sanjuán, R. Meucci, and F. T. Arecchi, *Chaos* **16**, 013111 (2006).
- [13] I. P. Mariño, E. Allaria, M. A. F. Sanjuán, R. Meucci, and F. T. Arecchi, *Phys. Rev. E* **70**, 036208 (2004).
- [14] A. Y. Loskutov and A. I. Shishmarev, *Chaos* **2**, 391 (1994).
- [15] K. A. Mirus and J. C. Sprott, *Phys. Rev. E* **59**, 5313 (1999).
- [16] K. T. Alligood, T. D. Sauer, and J. A. Yorke, *Chaos, an Introduction to Dynamical Systems* (Springer-Verlag, New York, 1996).
- [17] G. Tanaka, M. A. F. Sanjuán, and K. Aihara, *Phys. Rev. E* **71**, 016219 (2005).
- [18] W. H. Press, S. A. Teulolsky, W. T. Vetterling, and B. P. Flannery, *Numerical Recipes in C* (Cambridge University Press, Cambridge, 1988).
- [19] J. Hale and H. Koçak, *Dynamics and Bifurcations* (Springer-Verlag, Amsterdam, 1991).